Volume 18, No 1 | International Journal of Radiation Research, January 2020

Accuracy of empirical formulas in evaluation of neutron dose equivalent inside the ^{60}Co vaults reconstructed for medical linear accelerators

A. Ivković[1,2], D. Faj[1,3], S. Galić[4,5], A.H. Karimi[6], M. Kasabašić[1,2], H. Brkić[1,3*]

[1]Department of Biophysics and Radiology, Faculty of Medicine, J. J. Strossmayer University of Osijek, Croatia
[2]Department of Medical Physics, University Hospital Osijek, Croatia
[3]Department of Biophysics and Radiology, Faculty of Dental Medicine and Health, J. J. Strossmayer University of Osijek, Croatia
[4]Faculty of Medicine, University of Mostar, Bosnia and Herzegovina
[5]Department of Medical Physics, University Hospital Mostar, Bosnia and Herzegovina
[6]Department of Medical Physics, School of Medicine, Ahvaz Jundishapur University of Medical Sciences, Ahvaz, Iran

► ***Original article***

Corresponding authors:
Dr. Hrvoje Brkić,
E-mail: *hbrkic@mefos.hr*

Revised: October 2019
Accepted: November 2019

Int. J. Radiat. Res., January 2020; 18(1): 99-107

DOI: 10.18869/acadpub.ijrr.18.1.99

ABSTRACT

Background: In Southeast Europe medical accelerators are sometimes placed in small vaults originally built for ^{60}Co treatment unit. In order to meet shielding requirements for high energy photon beams, the wall thickness had to be increased. Since the vaults are already limited in size, instead of adding more concrete, materials with high-Z elements were used. Limited vault size and addition of high-Z elements can contribute to the neutron dose equivalent for both medical personnel and patients. ***Materials and Methods:*** The most commonly used empirical equations for estimation of neutron dose equivalent at the maze door in the vault are by Kersey and Wu-McGinley. In order to assess accuracy of these equations, Monte Carlo (MC) simulations of various geometrical and compositional changes of vault were conducted. Neutron ambient dose equivalent ($H^*_n(10)$) was observed when dimensions of the vault walls were reduced gradually. ***Results:*** The empirical equations gave results with reasonable accuracy when vaults were of standard size. When the vault was decreased to the size of the usual ^{60}Co unit vault, the most commonly used equations showed significant difference in results (up to 90%) in comparison to MC simulations. MC simulations showed that introducing different materials in shielding can change the neutron dose equivalent in vicinity of accelerators. ***Conclusion:*** For vaults limited in size, new simplified equation for neutron dose equivalent at the maze doors is presented, although performing a MC simulation of the specific vault is suggested.

Keywords: *LINAC, vault, Monte Carlo simulations, radiotherapy, neutron ambient dose equivalent.*

INTRODUCTION

High energy medical linear accelerators (LINACs) are widely used in radiation therapy (RT). Treatment of deeply seated tumors requires photon beams whose energy often exceeds 10 MeV. These photons interact with high-Z materials in the LINAC head and produce neutrons through Giant Dipole Resonance (GDR) reaction [1,2], consequently contaminating the therapeutic beam [3-6]. The neutron ambient dose equivalent ($H^*_n(10)$) in vicinity of the LINACs should be known and it has been the major interest of several recent experimental

[DOI: 10.18869/acadpub.ijrr.18.1.99]

and computational studies [3,4,7–10].

The neutron dosimetry is a very complex discipline, especially in the mixed fields, where the most accurate techniques cannot achieve uncertainties less than 10% [11]. These uncertainties are mainly due to the strong dependence of neutron detectors on neutron energy in the interval 0.1-5 MeV and saturation of neutron detectors by the photon flux [11,12]. Also, neutron dosimeters are expensive and therefore often inaccessible to medical physicists. That is why the empirical formulas are commonly used for estimation of $H^*_n(10)$ at the vault walls. Kersey and Wu-McGinley formulas [13,14] are the most frequently used in the shielding calculations since they are proposed by NCRP [8,9,15]. Both formulas were obtained by measuring $H^*_n(10)$ at the maze doors in series of already constructed vaults. Several studies have questioned the accuracy of the mentioned formulas, and found that both methods overestimate $H^*_n(10)$ in range of 1.14-3.8 times [16–20]. From radiation protection point of view, it is always better to overestimate than to underestimate the dose, because the underestimation can cause problems for the staff due to the insufficient protection and radiological problems. On the other hand, overestimation can impose additional costs and technical problems [18]. Also, studies have questioned various influences on $H^*_n(10)$, such as gantry orientation [21] and the vault construction geometry details [16]. New empirical equations are derived from these studies [16], but they don't give accurate results for accelerator vaults that significantly differ in size from simulated ones [16,21]. These formulas don't consider composition of the vault or addition of the materials that might contribute to neutron production or attenuation.

When accelerator is placed in vault with limited space, the wall thickness is often increased using high-Z materials (e.g. steel) [4]. Even though the steel attenuates photon and neutron flux, it becomes a new source of photoneutrons and makes the estimation of $H^*_n(10)$ more complicated and uncertain. If the vault is built within limited space, the maze is usually shorter [4] which often happens when vaults are reconstructed after decommissioning of ^{60}Co units. These vaults can be found in Southeast Europe and they present a problem for both medical personnel and patients. It is estimated that the medical personnel neutron dose reaches up to 2 mSv/year [4,6], which is higher than the photon contribution.

The aim of this study is to determine whether Kersey and Wu-McGinley equations [8,9,13,14] show agreement with the MC simulations of various vaults which differ in size and structure. The novelty in this study comes from separate changes in vault dimension and observation of their influence on $H^*_n(10)$. A new equation for estimation of $H^*_n(10)$ inside the maze of RT rooms will be proposed. The equation will be applicable to small vaults as well.

MATERIALS AND METHODS

MC model of 18MV LINAC Siemens Oncor has been constructed in MCNP6.1.1.beta® [22] code which has been tested in several previous publications [7, 23]. Simulated detectors were modeled as rectangular boxes in size of 10×10×10 cm^3 and they were set in the point on the inner side of maze doors. The F4 tally was assigned to each box and the neutron flux was converted to the $H^*_n(10)$ using ICRP 74 coefficients [24]. Both neutron source strength and $H^*_n(10)$ required for calculations of above-mentioned formulas were taken from our previous publication. Neutron source strength is 1.12×10^{12} neutrons per photon Gray at the isocenter and $H^*_n(10)$ is 2.4 mSv/Gy (for 10×10 cm^2 filed size) [7].

The model was built using macrobodies (mostly boxes and cylinders) predefined in MCNP and all simulations had at least 10^9 histories (electrons impinging on the target). Materials for the construction were taken from *Compendium of material composition data for radiation transport modeling* [25]. The rotation of the accelerator head was achieved using TRCL card in MCNP. In order to reduce the computational time and reduce errors, several variance reduction techniques were used. DXTRAN spheres were set within the detectors

[DOI: 10.18869/acadpub.ijrr.18.1.99]

and forced collisions in both vault and head materials were enabled. 10×10 cm² field was used in all simulations. Neutron spectra were collected in 56 energy bins ranging from 10^{-9} to 18 MeV in logarithmic scale which correspond to the ICRP [24] flux to dose conversion factors. The results were accepted when the relative error (R value) fell below 0.05, and all ten statistical checks were met. The energy cut-off for both electrons and photons was 1 keV, while for neutrons it remained 0 MeV. The continuous energy neutron cross sections library ENDF/B-VII (Evaluated Nuclear Data File B-VII) [26] was used for neutron transport.

Empirical methods for estimation of $H^*_n(10)$ at the maze entrance are the Kersey method [13] and the Kersey method modification given by Wu-McGinley [14].

The Kersey method states:

$$D_n = H_1 \cdot 10^{-3} \cdot \frac{A_r}{S_1} \cdot \frac{1}{d_1^2} \cdot 10^{\frac{-d_2}{5}} \quad (1)$$

where D_n is $H^*_n(10)$ at the maze entrance in mSv per photon dose at isocenter (Gy), H_1 is $H^*_n(10)$ at isocenter in mSv/X ray·Gy at the isocenter, A_r and S_1 are cross section area of entrance from maze to RT room and cross section of the maze respectively, both in square meters. d_1 is distance from isocenter to the maze and d_2 is distance from the door to the end of maze, both in meters.

Kersey method modification formula given by Wu-McGinley states [14]:

$$D_n = 2.4 \cdot 10^{-15} \phi_A \sqrt{\frac{A_r}{S_1}} \left(1.64 \cdot 10^{\frac{-d_2}{1.9}} + 10^{\frac{-d_2}{T_N}} \right) \quad (2)$$

where φ_A is total neutron fluence given by equation [27]:

$$\phi_A = \frac{Q_N}{4\pi d_1^2} + \frac{5.4 Q_N}{2\pi S} + \frac{1.26 Q_N}{2\pi S} \quad (3)$$

Q_N represents neutron source strength defined as number of neutrons coming from the head of treatment unit per X-ray dose (Gy) delivered at isocenter [28]. S represents surface of all RT room walls including floor and ceiling and is given in square meters and T_N is the tenth value length given as:

$$T_N = 2.06\sqrt{S_1} \text{ in meters.} \quad (4)$$

A template for the vault construction was obtained from the University Hospital in Osijek (figure 1). Vault construction details were changed by downsizing the vault until it reached the dimensions of the vault reconstructed after decommissioning the ^{60}Co unit and by enlarging it to dimensions found in literature [8,9,16]. The smallest vault used in this study was the vault reconstructed after decommissioning the ^{60}Co unit. It uses a very limited space (figure 2b) and it has been described previously together with $H^*_n(10)$ measurements [4].

Different scenarios were tested with the accelerator head pointed to the floor (figure 2):

a) The size of the vault was modified so that the walls were extended in steps of 1 m by increasing distance d_2 for the same amount. Five different sets of simulations were conducted, ranging from 1 to 5 m. The initial vault and maximum elongation are shown in the figure 2a.

b) The same dimension (as in case a) was contracted in 0.5 m steps, ranging from 0.5 to 1.5 m (figure 2b). The smallest vault has the size of the vault used in the University Hospital of Osijek.

c) Scenario b was modified by adding the steel panel (25 cm thickness) as a part of the vault wall (figure 2c). The steel was added only to vaults which are smaller than or equal to initial geometry.

All three previous scenarios were repeated, now with the accelerator head pointing in the direction of the additional steel wall.

d) The change in the cross section of the passage from the maze to the RT room (A_r) was tested so that the width was changed in the range from -0.5 (contraction) to 1.75 m (dilatation) in steps of 0.25 m (figure 2d)

e) The size of the maze corridor cross section (S_1) was changed so that the width of the corridor was increased in steps of 0.5 m ranging from 0.5 to 2.5 m (figure 2e).

[DOI: 10.18869/acadpub.ijrr.18.1.99]

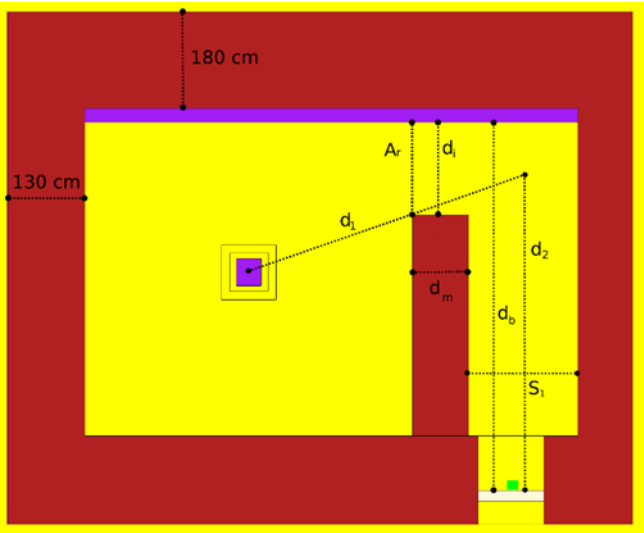

Figure 1. The ground plan of the starting structure of the vault. The concrete walls are shown in red, air inside the RT room is yellow, and the paraffin door is shown in white and the accelerator head in purple. The added steel wall is also represented in purple, and its thickness is 25 cm in all cases. Detector position is marked as green square. d^b represents length of the maze, d^i is width of the maze, S and A^r are cross sections of the maze RT room passage and the maze respectively. d^1 and d^2 are the distances between the isocenter and the inner maze point and between the detector and the inner maze point respectively, as defined in[9].

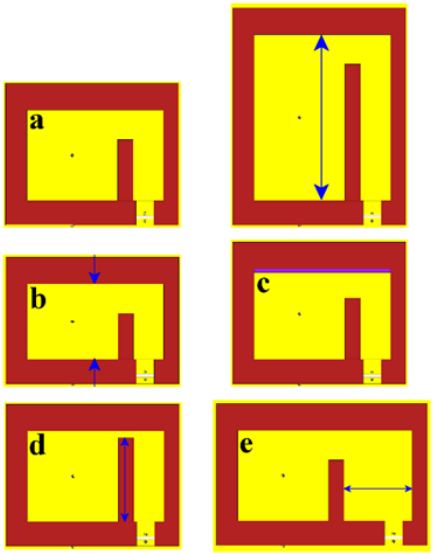

Figure 2. Ground plans for all simulated scenarios. Air is represented in yellow, concrete in dark red and additional steel barrier in purple: Blue arrows show direction of dimension change. a) Initial structure (maximum elongation on the right side), b) maximum contraction, c) addition of steel, d) maximum elongation of steel wall and e) maximum elongation of maze width.

RESULTS

Figure 3 compares $H^*_n(10)$ calculated by the Wu-McGinley formula (eq. 2), Kersey formula (eq. 1) and those obtained using MC for the a), b) and c) scenarios when the beam is pointed to the floor. Results of MC simulation of scenario in figure 2c are represented in figure 3 as well.

Figure 4 shows neutron spectra in the point near the vault door for the initial vault dimensions, with and without steel barrier. Figure 5 shows the scenario in which the accelerator head is rotated and the photon beam is pointed to the wall with steel plate, while the initial vault size has been contracted and expanded as in the scenarios with beam pointed to the floor.

The influence of maze length, orientation of the accelerator head and steel barrier insertion on neutron ambient dose equivalent was investigated in above presented scenarios. Furthermore, it was investigated how the neutron ambient dose equivalent was affected by the changes of the cross section of the passage between the RT room and the corridor (Ar) (scenario d)) as well as the changes of the cross section area of the corridor (S1) (scenario e)). The results are presented in figures 6 and 7.

MC simulations show that there is a very small influence of S_1 on the change of $H^*_n(10)$ at the maze, since it is almost constant. The Wu-McGinley method complies with this finding since it predicts that $H^*_n(10)$ at the maze will decrease with square root of S_1, but it underestimates the results for constant value as already seen in the figures 3 and 5. The Kersey method differs from our MC simulations significantly, since it predicts that the $H^*_n(10)$ at the maze will decrease with S_1.

Results obtained using these two methods differ up to 90% from our MC simulations in all simulated cases. The largest differences are in vaults with small dimensions. So, it seems reasonable to suggest a new formula which is going to include only the parameters and relations described earlier. The $H^*_n(10)$ depends

[DOI: 10.18869/acadpub.ijrr.18.1.99]

exponentially on d_2, linearly on change in A_r and change in S_1 could be omitted since $H^*_n(10)$ is almost constant upon its change. The modified equation states:

$$D_n = 3.43 \cdot 10^{-16} \cdot \phi_A \cdot e^{-\frac{d_2}{4.8}} \cdot A_r \qquad (5)$$

Figure 8 shows comparison of newly suggested formula with scenarios a), b) and c) while figure 9 shows comparison for scenarios d) and e).

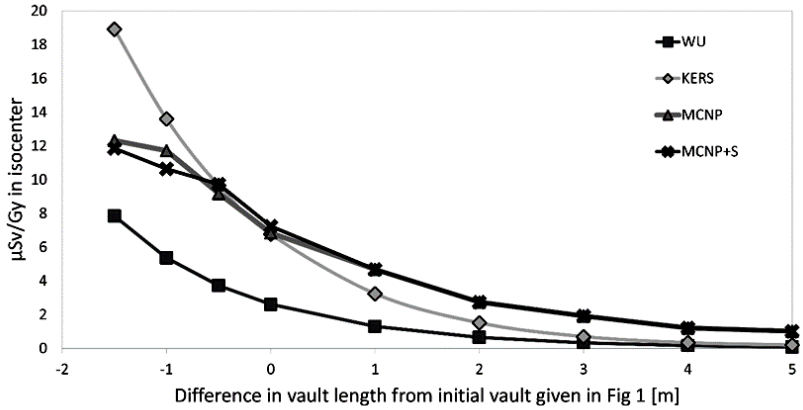

Figure 3. The comparison of (10) for the Wu-McGinley (WU), Kersey (KERS) formula and the MC data.The **a)**, **b)** and **c)** scenarios from figure 2 (the beam is pointed to the floor) with (MCNP+S) and without (MCNP) considering the steel barrier are shown.

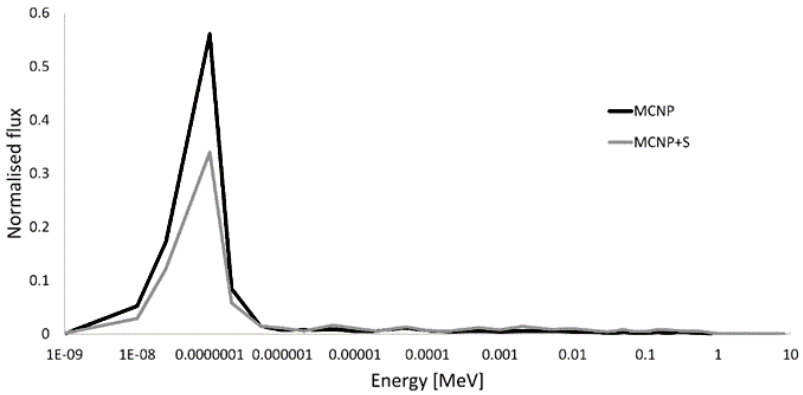

Figure 4. Neutron energy spectra for cases with (MCNP+S) and without (MCNP) steel barrier inserted as showed in figure 2c, normalized to the MCNP case.

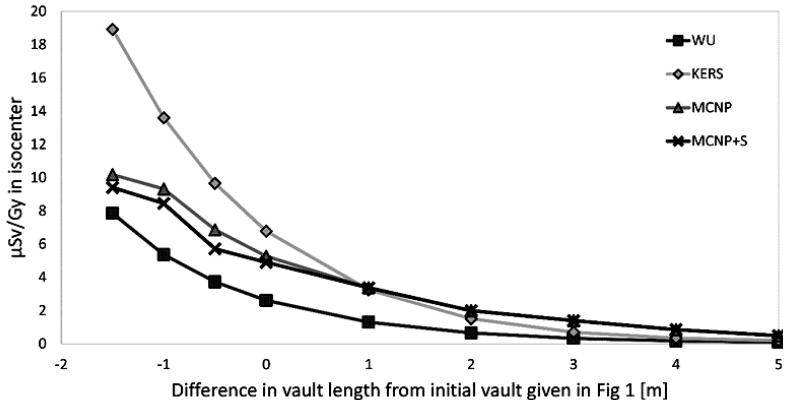

Figure 5. The comparison of (10) for the Wu-McGinley (WU), Kersey (KERS) formula and the MC data. The **a)**, **b)** and **c)** scenarios from figure 2 (the beam is pointed to the steel wall) with (MCNP+S) and without (MCNP) considering the steel barrier are shown.

[DOI: 10.18869/acadpub.ijrr.18.1.99]

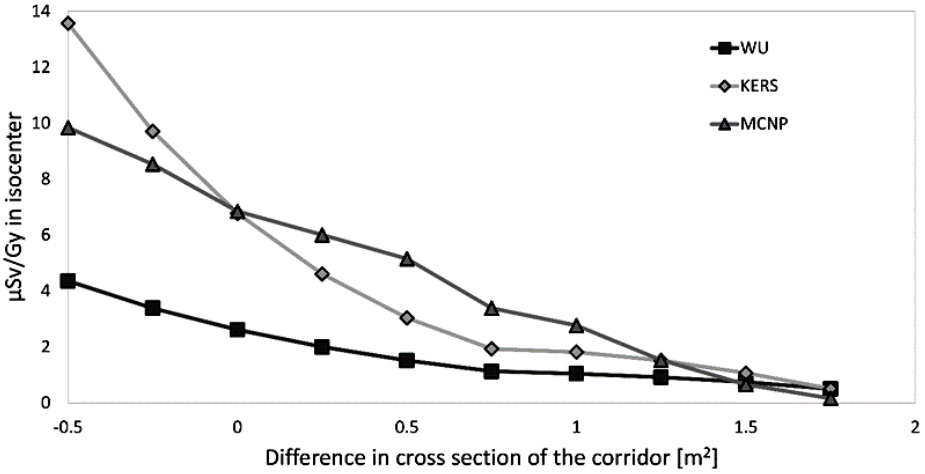

Figure 6. Change in neutron ambient dose equivalent $H^*_n(10)$ with the cross section area of the passage between RT room and corridor, Ar.

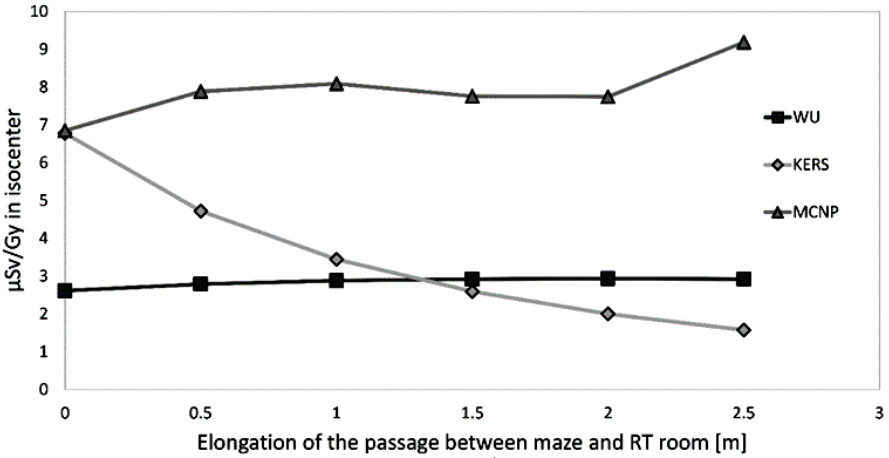

Figure 7. Change in neutron ambient dose equivalent $H^*_n(10)$ with the corridor cross section area (S1).

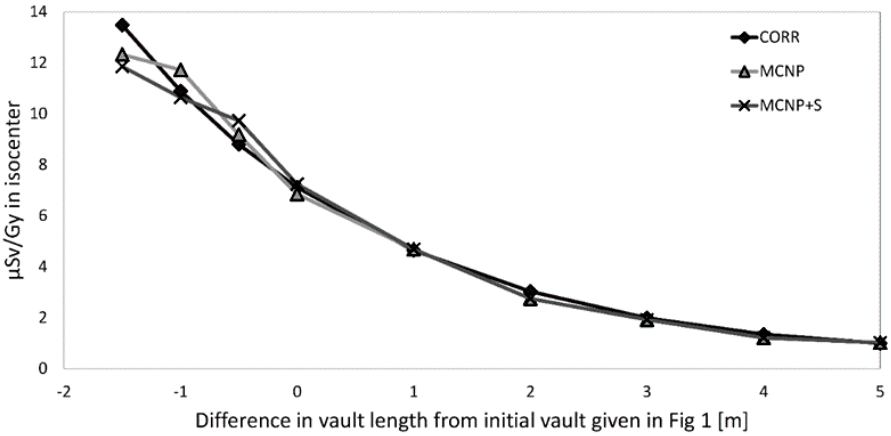

Figure 8. Comparison of MC simulation results and newly suggested formula for scenarios **a)**, **b)** and **c)** with and without steel barrier from figure 2. CORR presents the new empirical formula and MCNP computational results.

[DOI: 10.18869/acadpub.ijrr.18.1.99]

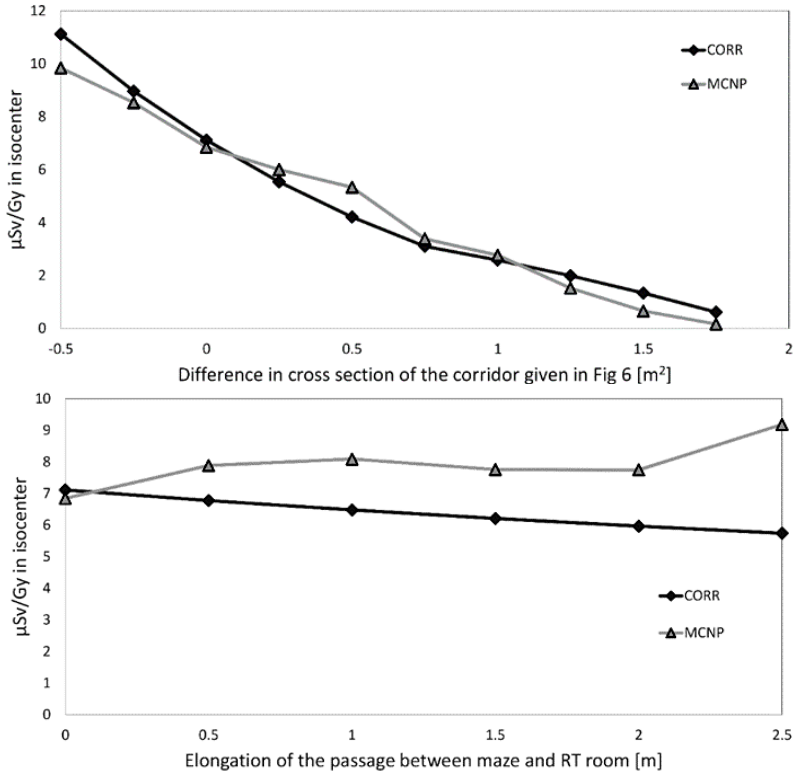

Figure 9. Comparison of MC simulation results and newly suggested formula for scenarios **d)** (up) and **e)** (down) from figure 2. CORR denotes results obtained with newly suggested formula, and MCNP denotes computational results.

DISCUSSION

The figure 3 shows that the $H^*_n(10)$ calculated using MC simulations decreases nearly exponentially with vault length increase. Commonly used empirical formulas [13,14] also predict the $H^*_n(10)$ in the maze with satisfying accuracy. By reducing the size of the vault, accuracy of the empirical formulas decreases, especially when Kersey method is used (eq 1). Wu-McGinley method (eq 2) gives better prediction for small vaults, though it underestimates the $H^*_n(10)$. The MC simulation of the vault with added steel panel, as in the figure 2c, shows that the steel insertion will decrease the $H^*_n(10)$ in the maze for approximately 10% (figure 3). Further MC investigation showed that the steel decreases neutron flux in the maze up to 30% in all cases. This means that the steel plate reduces the neutron contamination inside the maze, probably by attenuating the neutrons. Another interesting point is appearance of neutrons with higher energy after inserting the steel barrier (figure 4). Within this energy spectrum elastic scatter is the dominant interaction. Neutron mean path in steel and concrete are of the same order of magnitude, but average kinetic energy loss per collision is much smaller when neutrons interact with iron than any of elements in the concrete [29]. Moderating power of steel is much smaller than the moderating power of concrete for higher energies [29]. Steel plate reflects a portion of neutrons falling upon it. This process is the reason for excess of neutrons with higher energies coming from the accelerator head to the maze door (figure 4). Mean neutron energy without steel barrier was calculated to be 9.5 keV and with steel barrier 27 keV (initial structure). The next step was to find the origin of the neutrons coming to the maze. Using MC simulations it was estimated that the number of neutrons originated from the vault walls was less than 1% and those originated in the accelerator head more than 99% in all simulated cases without the steel barrier. When the steel barrier was inserted, simulations showed that the number of neutrons produced in the steel

[DOI: 10.18869/acadpub.ijrr.18.1.99]

barrier rose to nearly 10% of all neutrons coming to the maze. Such a result was expected since Fe (as a major element in the steel) has the noticeable energy threshold of 11.2 MeV for GDR process. The trend is similar in all simulated cases. Therefore, if a steel barrier is added in a vault, it will decrease the number of neutrons coming to the maze, but they will have higher energies.

Since the factor of conversion from neutron fluency to dose equivalent rises with energy, the dose equivalent difference between cases showed in the figure 3 is less than 20%. If the barrier I was thicker, placed differently (e.g. on the same wall but outside of vault), or in case of an additional barrier (e.g. on the wall between accelerator room and maze), the dose equivalent difference might change.

In the case when photon beam is pointed to the wall with steel barrier (figure 5), obtained curves are very similar to the case presented in the Fig 3 when beam is pointed to the floor. Nevertheless, the Wu-McGinley method now describes the behavior of $H^*_n(10)$ very well. When adding a simple correction factor to the Wu-McGinley curve, MCNP and WU curves match. According to our MC results, the change of the $H^*_n(10)$ with A_r is close to linear while both empirical formulas predict different behavior (figure 6).

Results shown in figure 8 suggest that our modified formula (eq 5) shows $H^*_n(10)$ overestimation of 20% in the worst-case scenario. It is reasonable to assume that it would show even higher discrepancy for bigger contraction, but vaults of that size are unlikely to be built. Figure 9 suggests that the new formula predicts the influence of change in cross section of the passage between RT room and maze on $H^*_n(10)$ very well. Even if the S_1 is omitted from the new formula, discrepancy between prediction and MC is not higher than 20%.

CONCLUSION

This study reinvestigated two mostly used empirical methods for $H^*_n(10)$ estimation in vault mazes of the LINACs. The main interest was in vaults built within small spaces since there are very few investigations of such situations. When the vault has to be built in a limited space and especially if high-Z materials barriers are used, there is a significant possibility of high doses in vaults and surrounding spaces. Therefore, we recommend the investigation of the neutron fluency by MC simulations or measurements. If such methods are not available, we recommend the use of our new empirical formula since in these cases the Wu-McGinley method underestimates $H^*_n(10)$ significantly.

ACKNOWLEDGMENTS

This study was financed by J. J Strossmayer University project ZUP2018-16.

***Conflicts of interest*:** *Declared none.*

REFERENCES

1. Esposito A, Bedogni R, Lembo L, Morelli M (2008) Determination of the neutron spectra around an 18 MV medical LINAC with a passive Bonner sphere spectrometer based on gold foils and TLD pairs. Radiat Meas. *Elsevier, **43(2–6)** :1038–43*.
2. Vega-Carrillo H, Hernández-Almaraz B, Hernández-Dávila V, Ortíz-Hernández A (2009) Neutron spectrum and doses in a 18 MV LINAC. *J Radioanal Nucl Chem, Akadémiai Kiadó, co-published with Springer Science+ Business Media BV …; **283(1)**: 261–5*.
3. Karimi AH, Brkić H, Shahbazi-Gahrouei D, Haghighi SB, Jabbari I (2019) Essential considerations for accurate evaluation of photoneutron contamination in Radiotherapy. *Appl Radiat Isot, **145**: 24–31.*
4. Poje M, Ivković A, Jurković S, Žauhar G, Vuković B, Radolić V, *et al.* (2014) The neutron dose equivalent around high energy medical electron linear accelerators. N*ucl Technol Radiat Prot, **29(3)**: 171–8*.
5. Schraube H, Kneschaurek P, Schraube G, Wagner FM, Weitzenegger E (2002) Neutron spectra around medical treatment facilities. *Nucl Instruments Methods Phys Res Sect A Accel Spectrometers, Detect Assoc Equip, **476(1)**: 463–7*.
6. Vukovic B, Faj D, Poje M, Varga M, Radolic V, Miklavcic I, *et al.* (2010) A neutron track etch detector for electron linear accelerators in radiotherapy. *Radiol Oncol, **44(1)**: 62*

[DOI: 10.18869/acadpub.ijrr.18.1.99]

–6.
7. Brkić H, Ivković A, Kasabašić M, Poje Sovilj M, Jurković S, Štimac D, *et al.* (2016)The influence of field size and off-axis distance on photoneutron spectra of the 18 MV Siemens Oncor linear accelerator beam. *Radiat Meas,* ***93****: 28–34*.
8. Aono Y, Higashisaka A, Ogawa T (2006) NCRP Report 151 Structural shielding design and evaluation for megavoltage X-and gamma-ray radiotherapy facilities*. NCRP report 115, Bethesda, MD, USA.*
9. IAEA 47 IAE. Radiation protection in the design of radiotherapy facilities. Internat. Atomic Energy Agency; 2006.
10. Maglieri R, Licea A, Evans M, Seuntjens J, Kildea J (2015) Measuring neutron spectra in radiotherapy using the nested neutron spectrometer. *Med Phys, Wiley Online Library,* ***42(11)****: 6162–9*.
11. Chibani O and Ma C-MC (2003) Photonuclear dose calculations for high-energy photon beams from Siemens and Varian linacs. *Med Phys,* ***30(8)****: 1990–2000*.
12. Zabihinpoor S and Hasheminia M (2011) Calculation of Neutron Contamination from Medical Linear Accelerator in Treatment Room. *Adv Stud Theor Phys,* ***5(9)****: 421–8*.
13. Kersey RW (1979) Estimation of neutron and gamma radiation doses in the entrance mazes of SL75-20 linear accelerator treatment rooms. *Med Mundi,* ***24****: 151–5*.
14. Wu RK and McGinley PH (2003) Neutron and capture gamma along the mazes of linear accelerator vaults. *J Appl Clin Med Phys,* ***4(2)****: 162–71*.
15. NCRP, National Council on Radiation Protection and Measurements (2009) Ionizing radiation exposure of the population of the United States. *NCRP Report No. 160 . NCRP, Bethesda, MD*.
16. Kim H, Jang K, Park Y, Kwon J, Choi H, Lee J, *et al.* (2009) New empirical formula for neutron dose level at the maze entrance of 15 MV medical accelerator facilities. Wiley Online Library; *Med Phys,* ***36(5)****: 1512–20*.
17. Wang X, Esquivel C, Nes E, Shi C, Papanikolaou N, Charlton M (2011) The neutron dose equivalent evaluation and shielding at the maze entrance of a Varian Clinac 23EX treatment room. Wiley Online Library; *Med Phys,* ***38(3)****: 1141–9*.
18. Beigi M, Afarande F, Ghiasi H (2016) Safe bunker designing for the 18 MV Varian 2100 Clinac: a comparison between Monte Carlo simulation based upon data and new protocol recommendations. *Reports Pract Oncol Radiother*, ***21(1)****: 42–9*.
19. Ramírez PVC, Góngora JAID, Gutiérrez LCP, Montalvo TR, Carrillo HRV (2016) Neutron H*(10) estimation and measurements around 18 MV linac. *Appl Radiat Isot,* ***117****: 2–7*.
20. Mesbahi A, Ghiasi H, Mahdavi SR (2010) Photoneutron and capture gamma dose equivalent for different room and maze layouts in radiation therapy. *Radiat Prot Dosimetry,* ***140(3)****: 242–9*.
21. Ghiasi H and Mesbahi A (2012) Gantry orientation effect on the neutron and capture gamma ray dose equivalent at the maze entrance door in radiation therapy. *Nucl Technol Radiat Prot,* ***27(1)****: 70–4*.
22. Goorley JT (2014) MCNP6. 1.1-Beta release notes Los Alamos National Laboratory Technical Report. *LA-UR-14-24680.*
23. Brkić H, Kasabašić M, Ivković A, Agić D, Krpan I, Faj D (2018) Influence of head cover on the neutron dose equivalent in Monte Carlo simulations of high energy Medical linear accelerator. *Nucl Technol Radiat Prot,* ***33 (2)****: 217–22*.
24. ICRP (1996) Conversion coefficients for use in radiological protection against external radiation. *Ann ICRP,* ***26****: 3–4*.
25. McConn RJ, Gesh CJ, Pagh RT, Rucker RA, Williams III R (2011) Compendium of material composition data for radiation transport modeling. Pacific Northwest National Laboratory (PNNL), Richland, WA (US).
26. Chadwick MB, Obložinský P, Herman M, Greene NM, McKnight RD, Smith DL, *et al.* (2006) ENDF/B-VII. 0: next generation evaluated nuclear data library for nuclear science and technology. *Nucl data sheets,* ***107(12)****: 2931–3060*.
27. McCall RC, McGinley PH, Huffman KE (1999) Room scattered neutrons. Wiley Online Library; *Med Phys,* ***26(2)****: 206–7*.
28. NCRP60 60 (1984). Neutron Contamination from Medical Electron Accelerators: Recommendations of the National Council on Radiation Protection and Measurements. Ncrp Report 60, Bethesda, MD, USA; **(79)**.
29. Rinard P (1991) Neutron interactions with matter. Passiv Nondestruct Assay Nucl Mater. US Nuclear Regulatory Commission NUREG/CR-5550; *(375–377)*.

[DOI: 10.18869/acadpub.ijrr.18.1.99]